Central European Geology, Vol. 61/2, 85–108 (2018)
DOI: 10.1556/24.60.2017.013
First published online January 18, 2018

Metamorphic and deformation history of the Mecsekalja Zone around the Szentlőrinc-1 well using individual quartz grains from drilling chips

Ágnes Skultéti[1]*, Tivadar M. Tóth[1], István János Kovács[2], Edit Király[3], Judit Sándorné Kovács[4]

[1]Faculty of Science and Informatics, Department of Mineralogy, Geochemistry and Petrology, University of Szeged, Szeged, Hungary
[2]MTA Research Centre for Astronomy and Earth Sciences, Geodetic and Geophysical Institute, Sopron, Hungary
[3]Department of Geochemistry and Laboratories, Mining and Geological Survey of Hungary, Budapest, Hungary
[4]Department of Physics and Chemistry, Hungarian Institute for Forensic Sciences, Budapest, Hungary

Received: December 16, 2016; accepted: October 24, 2017

The Mecsekalja Zone is a strike-slip fault zone that plays an essential role in the structural framework of South Transdanubia. The metamorphic and deformation history of the crystalline basement of the Mecsekalja Zone has been determined thus far based exclusively on a few surface outcrops and near-surface samples. The Szentlőrinc-1 (Sztl-1) well penetrated the shear zone at a depth of approximately 2 km and brought drilling chips from a 220-m-long section of the basement to the surface. The aim of this study is to reconstruct the metamorphic and deformation history of the Mecsekalja Zone along the Sztl-1 well using these tiny samples. These drilling chips consist of single mineral and rock pieces that are dominated by quartz grains. This study concentrates on the detailed analysis of quartz grains utilizing the physical conditions of metamorphic evolution as well as ductile and brittle deformation to determine the chemical composition and rheology of quartz. The evolution of the studied area can be determined by evaluating analytical data measured by Raman spectroscopy, LA-ICP-MS, and FTIR spectroscopy. These data suggest that the maximum temperature of the early regional metamorphism was 500–575 °C, the temperature of the subsequent ductile deformation was below 500 °C including recrystallization occurred between 400 and 475 °C. During the structural evolution of the study area, two independent, single deformation events occurred. The earlier ductile deformation event was followed by a brittle event through the reactivation of the former ductile shear zone. Our model is in accordance with previous results concerning the evolution of the Mecsekalja Zone, thus, the shear zone, with an identical evolution, can be extended toward the southwest at least to the Sztl-1 well.

Keywords: Mecsekalja zone, gneiss, quartz, metamorphism, deformation, TitaniQ thermometer

*Corresponding author: Ágnes Skultéti; Faculty of Science and Informatics, Department of Mineralogy, Geochemistry and Petrology, University of Szeged, Egyetem utca 2., Szeged H-6722, Hungary
E-mail: skulteti.agi@gmail.com

ISSN 1788-2281 © 2017 *The Author(s)*

Introduction

The Mecsekalja Zone is a ~1.5-km-wide strike-slip fault zone in South Transdanubia, Hungary (Fig. 1) that has been active since the Permian and that significantly controls the structural evolution of the adjacent areas (Szederkényi 1977). In the dislocation zone, intensively mylonitized metamorphic rocks of various lithologies crop out. Gneiss, quartz phyllite, crystalline limestone, serpentinite, and amphibolite compose the Mecsekalja Zone and lithostratigraphically belong to the Ófalu Group. Previously, the metamorphic and deformation history of these rock types was studied basically from surface outcrops (Szederkényi 1977, 1983; Árkai and Nagy 1994; Lelkes-Felvári et al. 2000; Király and Török 2003; M. Tóth et al. 2005, Balla et al. 2009, among others). Recently, the Szentlőrinc-1 (Sztl-1) well reached the basement SW of the well-known surface outcrops at a depth of approximately 2 km

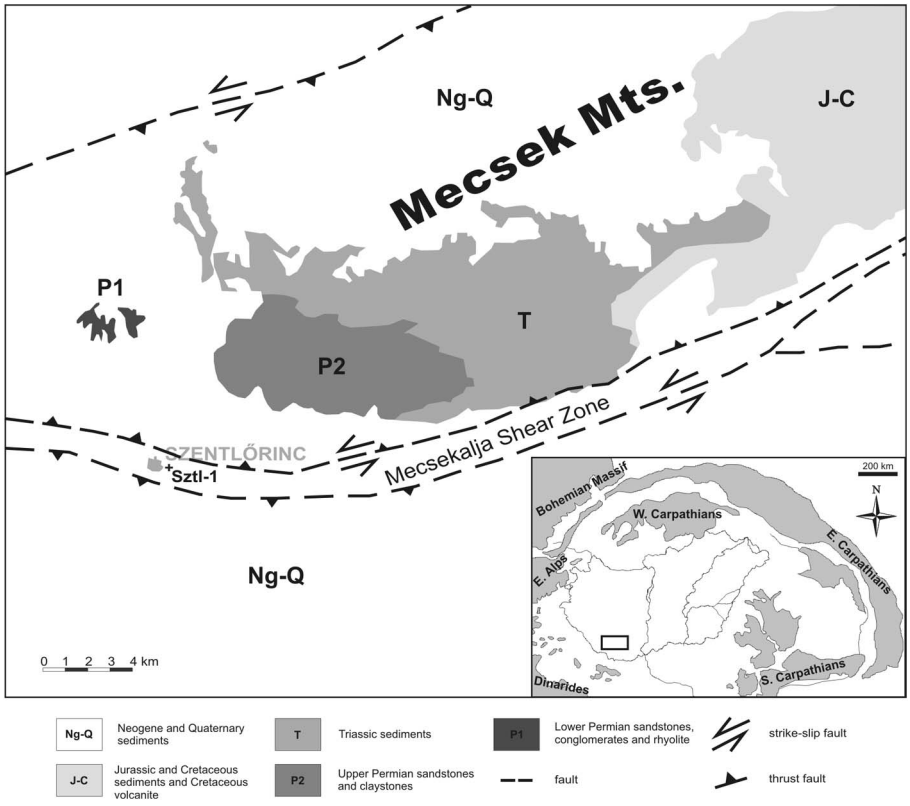

Fig. 1
The Mecsekalja Zone with the studied Szentlőrinc-1 (Sztl-1) well (based on Konrád et al. 2010)

and brought drilling chips to the surface, thus making it possible to investigate the shear zone. These drilling chips consist of mm-sized debris and contain single mineral and rock pieces in an 80:20 ratio; these pieces are dominated by quartz grains.

Quartz, which is one of the most frequent rock-forming minerals, is a common product of metamorphic reactions. In its crystal lattice, various trace elements (e.g., Al, Ti, Ge, Na, K, Li, and B) (Götze et al. 2004) may appear connected to SiO_4 tetrahedrons under different physical conditions; thus, metamorphic evolution determines the chemical composition of quartz (Monecke et al. 2002; Sørensen and Larsen 2009; Kempe et al. 2012). Although quartz is a "nominally anhydrous mineral," in its crystal lattice, hydrogen ("water") may occur both in the form of hydroxyl defects (OH^-) and molecular water (H_2O) (Stenina 2004). Hydroxyl defects in the quartz lattice are mostly locked in crystal defects (point defects) and along grain boundaries, whereas molecular water appears freely in the form of fluid (nanoscale) inclusions (Stadler and Konzett 2012).

The amount of "water" in the crystal lattice of quartz significantly influences its brittle and ductile behavior reduces its mechanical strength and resistivity and enhances its ductile deformation at low temperatures (200–300 °C; Griggs and Blacic 1965; Blacic 1975; Jones 1975; Kekulawala et al. 1978, 1981; Gleason and DeSisto 2008). All these factors indicate that quartz is an excellent candidate for recording metamorphic evolution and structural changes in numerous rock types. Because quartz is a stable mineral over a rather wide range of *P–T* conditions, it can be deformed in different ways due to diverse deformation mechanisms to produce various microstructures (Hirth and Tullis 1992; Passchier and Trouw 2005). Consequently, each grain in a quartz-bearing rock may provide valuable information regarding the deformation history of the rock body itself (Stipp et al. 2002; Vernon 2004; Halfpenny et al. 2012).

The aims of this study are to reconstruct the metamorphic and deformation history of the Mecsekalja Zone around the Sztl-1 well using quartz grains of drilling chips and to compare our data with the previous evolutionary models of the study area.

Geological setting

Geology of the Mecsekalja Zone

The Mecsekalja Zone consists of rocks that originally belonged to distinct stratigraphic and tectonic units (Balla 2003a; Balla et al. 2009). The Palaeozoic rocks of the Ófalu Group were most likely juxtaposed along a regional ductile strike-slip zone (Mecsekalja Zone) during the main Early Carboniferous orogenic phase of the Variscan cycle (Balla et al. 2009). Rock types of the Ófalu Group, including gneiss, amphibolite, crystalline limestone, quartz phyllite, and serpentinite, represent the intensively deformed pieces of these stratigraphic and structural units (Balla 2003b).

The protolith of the highly mylonitic gneiss was presumably a granitoid rock, therefore classifying it as an orthogneiss (Király 2005; M. Tóth et al. 2005). Previous examinations by M. Tóth et al. (2005) indicated that the zircon grains of the Mórágy Granite differ from those typically found in the Ófalu gneiss mylonite. Thus, its protolith cannot be the Mórágy Granite but is instead another, currently unknown granitoid rock. The age of this protolith must be older than the Mórágy Granite (Klötzli et al. 2004; M. Tóth et al. 2005), therefore, older than Early Carboniferous. Szederkényi (1977, 1983) suggests that the protolith of amphibolite is partly volcanogenic and volcanogenic-sedimentary. The crystalline limestone has been identified as a metamorphic variety of a Devonian limestone based on the presence of conodonts as described by S. Kovács (personal communication).

The earliest detected event of the evolution of the crystalline basement is the magmatic crystallization of quartz grains in gneiss protolith granitoid rocks. This event occurred at ~710 °C based on quartz suture analysis performed by M. Tóth et al. (2005). Zoned garnet composition (specifically, increasing Mg and decreasing Fe contents from core to rim, Lelkes-Felvári et al. 2000) and quartz suture data of M. Tóth et al. (2005) suggest that the first regional metamorphic event occurred at upper greenschist/lower amphibolite facies (~550 °C) in both the gneissic rocks and amphibolite. Greenschist/amphibolite facies metamorphism in amphibolite was described by Szederkényi (1977, 1983) and has been confirmed by the cores of zoned amphibole porphyroclasts from Erdősmecske (~540 °C, 3.2 kbar, Árkai and Nagy 1994). As the crystalline limestone also metamorphosed at high-*T* greenschist facies, the age of this metamorphic event must be younger than the Devonian (Balla et al. 2009).

In the different rock types of the Ófalu Group, intensive ductile deformation is associated with this metamorphic event, leading to multiphase folding and intensive mylonitization. Based on the mineral composition of ultramylonite of the Mőcsény-I borehole, Lelkes-Felvári et al. (2000) estimated that high-*T* greenschist facies (~450 °C) mylonitization occurred under medium (Barrow-type) pressure conditions. Király and Török (2003) estimated that the temperature of this mylonitization was approximately 450–500 °C based on garnets in deformed aplite. Szederkényi (1977, 1983) described intensive shearing at greenschist/amphibolite facies in amphibolite, whereas M. Tóth et al. (2005) assumed the recrystallization temperature of mylonite to be approximately 350 °C. The $^{40}Ar/^{39}Ar$ muscovite age of the mylonite is 270–303 Ma (Lelkes-Felvári et al. 2000), although Tüske (2001) proposed an age of 294–307 Ma for ductile shearing based on $^{40}Ar/^{39}Ar$ dating of biotite and muscovite from a mylonitic biotite gneiss.

Previous results from the Sztl-1 well

Petrography. In the drilling chips of the Szentlőrinc-1 well, in addition to quartz, rock grains, which consist of muscovite, biotite, K-feldspar, and plagioclase, are also present. In the upper 100–150 m of the studied well section, muscovite and K-feldspar are the prevailing phases, with mica dominance; further downward, the

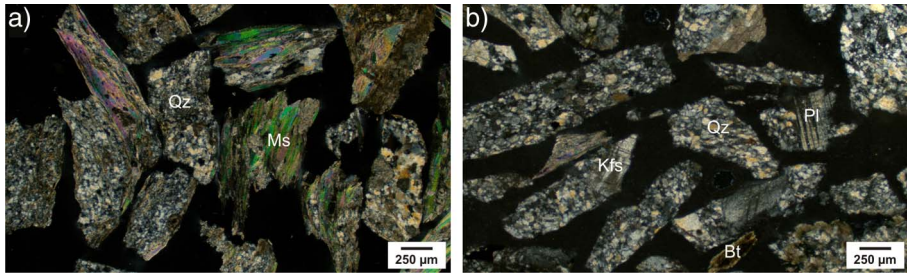

Fig. 2
Different gneiss types along the studied well section (1,600–1,820 m) of the Sztl-1 well. (a) Micaceous gneiss with dominant quartz (Qz) and muscovite (Ms) and (b) feldspathic gneiss with dominant quartz (Qz), K-feldspar (Kfs), plagioclase (Pl), and biotite (Bt)

amount of plagioclase increases, and biotite also appears. Thus, the studied well section can be divided into two blocks of different gneiss types (Fig. 2): the upper micaceous gneiss (Fig. 2a) and the lower feldspathic gneiss (Fig. 2b) (Skultéti and M. Tóth 2016).

Ductile and brittle deformation. Three microstructurally distinct quartz grain types (Fig. 3) in the subsurface shear zone were distinguished under a polarizing microscope: grains with undulose extinction (Fig. 3a), grains with subgrains (Fig. 3b), and grains of recrystallized grains (Fig. 3c), denoted as U (undulatory), S (subgrain), and R (recrystallized), respectively. In addition, numerous grains with heterogeneous microstructures (Fig. 3d) were also observed. These transitional features exhibit the simultaneous presence of more end-member structure types within a single grain (Skultéti et al. 2014; Skultéti and M. Tóth 2016).

Textural evidence indicates that the U-type quartz grains were formed via bulging recrystallization (BLG) (Hirth and Tullis 1992). Bulging usually occurs at low temperatures (~400 °C) (Passchier and Trouw 2005) and high strain rates. In contrast, the S- and R-type quartz grains probably developed via subgrain rotation recrystallization (SGR) (Hirth and Tullis 1992) at different temperature ranges (SGR I ~450 °C, SGR II ~500 °C) (Skultéti et al. 2014). The latter process generally occurs at medium temperatures (~500 °C) and strain rates (Passchier and Trouw 2005). Thus, these three end-member microstructural types were formed by two different mechanisms (namely BLG and SGR) representing distinct deformation conditions.

Using Raman microspectroscopy, monomineralic quartz domains developed under different deformation conditions can be identified and separated. Statistical analysis indicates that the microscopically identified end-member grains (U, S, and R) possess significantly different spectral attributes; thus, they can be distinguished based on certain combinations of their respective Raman spectra (*F1, F2*

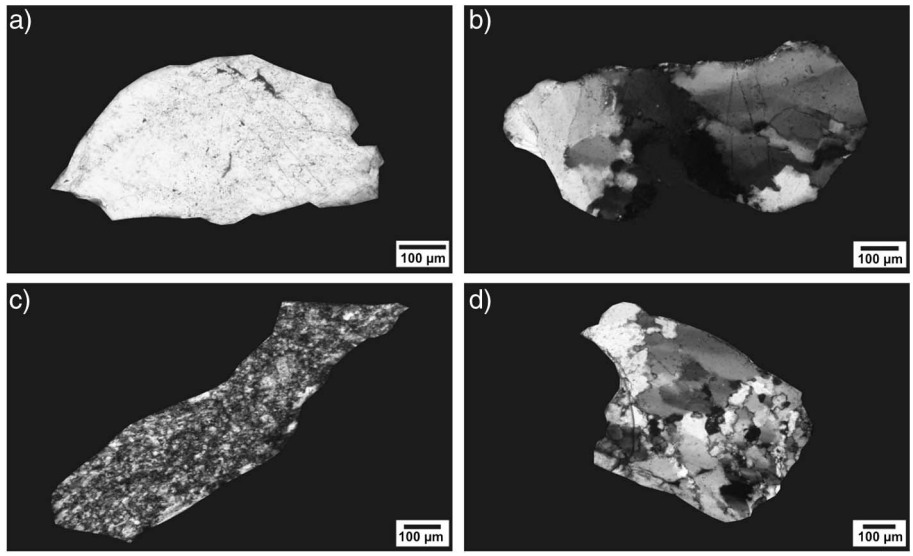

Fig. 3
Microstructural groups of quartz grains in the studied samples. (a) Quartz grain with undulose extinction (U), (b) quartz grain with subgrains (S), (c) quartz grain with recrystallized grains (R), and (d) transitional quartz grain with heterogeneous microstructures

discriminant functions in Skultéti et al. 2014) (Fig. 4). The U–S–R spectral space (or the U–S–R "triangle") can therefore also be considered to represent a virtual deformational space.

Based on the microstructures and recrystallized grain sizes (45 ± 20 µm) (Stipp et al. 2002) of quartz grains, the maximum temperature of ductile deformation of the samples from the Sztl-1 well was below 500 °C (Skultéti et al. 2014). Throughout the well, the proportion of microstructurally distinct quartz grains changes with depth (Skultéti and M. Tóth 2016). Thus, based on these investigated samples, ductile shear zones can be localized at depths of approximately 1,610–1,635 and 1,750–1,765 m (Fig. 5) (Skultéti and M. Tóth 2016). In addition, two brittle shear zones can be identified by manual and statistical (discriminant analysis) interpretations of well logs (density, gamma, resistivity, spontaneous potential, and calliper logs) at depth intervals of approximately 1,580–1,635 and 1,750–1,765 m (Fig. 5).

Geodynamics. The positions of the ductile shear zones coincide very well with the brittle horizons defined by well-log evaluations (for details, see Skultéti and M. Tóth 2016). This behavior may suggest two different evolution schemes for the Mecsekalja Zone (Skultéti and M. Tóth 2016). (a) If the first evolved ductile shear zones produced softened regions inside the crystalline mass, then they could

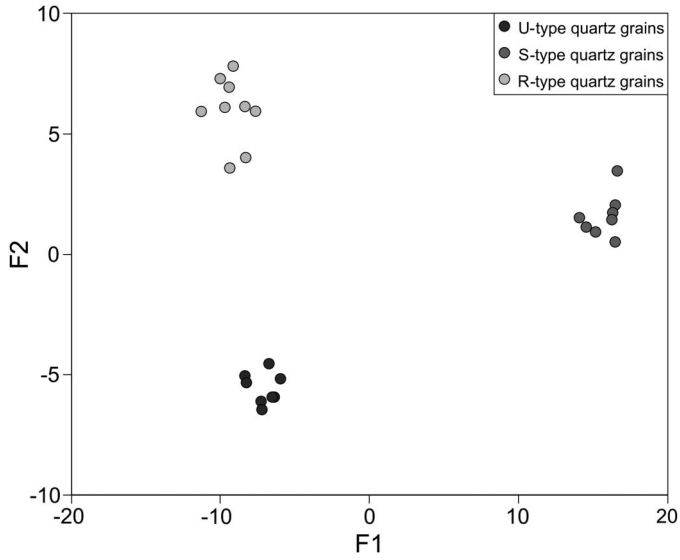

Fig. 4
Separation of U–S–R end-member quartz grain types in the spectral space using Raman spectroscopy on the basis of *F1, F2* discriminant functions

reactivate later in a brittle manner due to a tectonic event independent of the early one, similar to that described by White et al. (1986) and Holdsworth et al. (1997). (b) If these structures formed due to the same tectonic event, then these zones may represent a detachment fault (Lister et al. 1986; Davis 1988). Detachment faults develop as the result of continental extension when the middle and lower continental crust, which was previously deformed in a ductile manner, is uplifted to the brittle upper crust (Lister and Davis 1989). Consequently, ductile and brittle deformation overlaps along the same shear zones that separate blocks of different metamorphic evolutions.

Samples

This study area is located in the South Transdanubian region of Hungary and is part of the Mecsekalja Zone at the forefront of the Mecsek Mountains. The investigated samples represent the Sztl-1 deep drilling well (Thorbergsdottir et al. 2010), the base of which reached a depth of 1,820 m. Under Cenozoic and Mesozoic sedimentary formations, the well-penetrated rocks of the Mecsekalja Shear Zone. Drilling chips were obtained at every 5 m in 1,600–1,820 m interval (analyzed samples are from depths of 1,605, 1,620, 1,635, 1,660, 1,675, and 1,770 m).

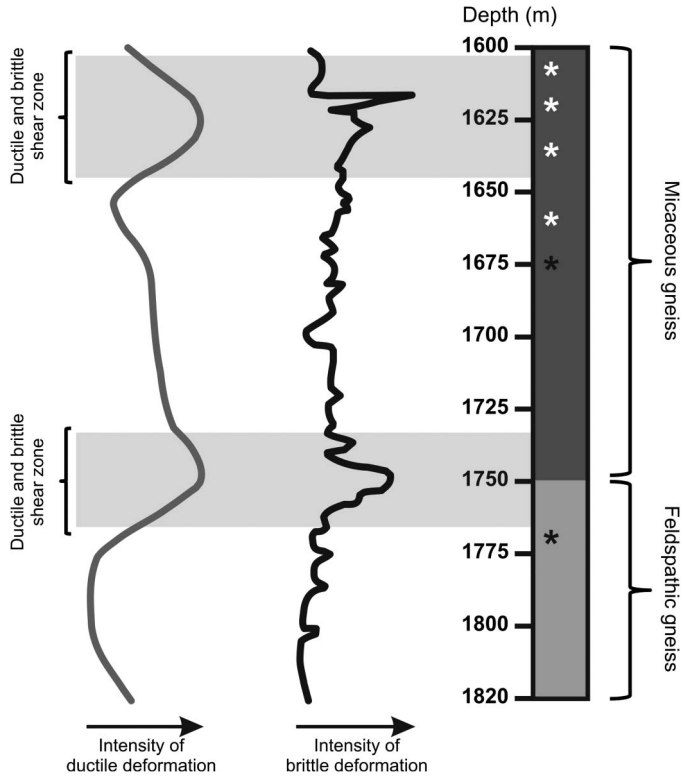

Fig. 5
Position of ductile (gray line) and brittle (black line) shear zones in the studied section of the Sztl-1 well (Skultéti and M. Tóth 2016). White stars represent the position of the samples used for micro-FTIR measurements, whereas black stars represent the position of the samples used for Raman spectroscopy and LA-ICP-MS measurements

Methods

Raman spectroscopy

Measurements were performed on 100-μm thick sections, so that these samples could be used for further analysis. This sample thickness hinders the optical analysis of quartz grains; therefore, Raman spectroscopy was used for the detailed study of quartz microstructures. In the samples obtained from depths of 1,675 and 1,770 m (Fig. 5), 10 random points were measured in each selected end-member or transitional quartz grain. Based on the resulting Raman spectral attributes, the analyzed quartz grains were situated in the *F1–F2* spectral space and in the U, S, and R "triangle."

Analyses were performed on a Thermo Scientific DXR Raman microscope equipped with a diode-pumped frequency-doubled Nd-YAG laser at a maximum laser power of 10 mW. Samples were irradiated by laser light at a wavelength of 532.2 nm, with the laser beam focused using a 100× objective lens, resulting in a spot size of ca. 0.7 μm. The backscattered light collected by the microscope objective was filtered via an edge filter, dispersed by a single grating (1,800 grooves mm^{-1}) and gathered in a CCD detector cooled to −20 °C by the Peltier effect. This instrument has a spectral resolution better than 2 cm^{-1} and a spatial resolution of a few μm^3; a 50-μm pinhole confocal aperture was used for each measurement. In every case, 10 mW laser power was used to record the spectra. Sample exposures were obtained by operating the DXR Raman microscope in autoexposure operating mode, in which the instrument attempts to reach a specified signal-to-noise ratio (*S*/*N*) during the measurement (in this case, $S/N = 100$). In this measuring mode, a maximum exposure time must also be set (i.e., if the specified *S*/*N* value cannot be achieved); a value of 1 min was set for each spectrum selected in this study. The applied Raman microscope was equipped with a laser source operating with a depolarized laser beam. Due to the depolarized nature of the applied laser beam, the directional dependence of the Raman scattering did not influence the quality of the recorded spectra. Seasolve PeakFit 4.12 software was used for Raman spectral analysis. A Gaussian deconvolution method using the Voight-type curve fitting procedure was used to determine the center, amplitude, full width at half-max (FWHM), full width at base (FWHM base), and integrated area of the bands of interest.

Laser ablation inductively coupled plasma mass spectrometry (LA-ICP-MS)

Measurements were performed using a New WaveUP 213 laser ablation system coupled to a quadrupole ICP-MS, Perkin Elmer Elan DRCII, at the Geological and Geophysical Institute of Hungary. He carrier gas was mixed with Ar gas, which acted as a make-up gas. Operating parameters of the ICP-MS and laser ablation system were optimized using NIST612 as the unknown material and NIST610 as the control. Conditions of the mass spectrometer are characterized by a nebulizer gas of 0.9 L/min, auxiliary gas of 1.1 L/min, plasma gas of 15.8 L/min, lens voltage of 7.25 V, and RF power of 1,450 kW. The He gas flow was as high as 1.8 L/min. The laser operated at an energy density of 4.7 J/cm^2 and a repetition rate of 5 Hz. The spot size was 55–100 μm. The background acquisition time was 40 s, and the sample signal was measured over 60 s. The total integration time for each isotope was 13 s. NIST610 was used as an external standard, and ^{29}Si was used as an internal standard. Absolute concentrations were calculated to 100% of SiO_2 measured simultaneously on the same spot by LA-ICP-MS (Liu et al. 2008).

These measurements were made on 100-μm-thick polished sections. Measured quartz grains were selected by detailed Raman spectroscopy analysis. The concentration of ^{49}Ti in quartz grains in two samples from different depths (1,675 and 1,770 m; Fig. 5) was determined by LA-ICP-MS. In total, 14 quartz grains were

analyzed, and 50 measurements were performed on two samples. In the sample collected from a depth of 1,675 m, 33 points from nine quartz grains were measured; in the sample collected from a depth of 1,770 m, 17 points from five quartz grains were measured. The intensity versus time signal was also checked for spikes and inclusions. To ensure good representation and to avoid accidental contamination of anatase inclusions or any other mineral forming on the grain boundary, 3 points per grain were measured, and the average was used to calculate the temperature, if their deviation was small enough.

Temperatures were calculated from the measured Ti concentrations using a Ti-in-quartz thermometer (TitaniQ) of Thomas et al. (2010):

$$T(^{\circ}\mathrm{C}) = \frac{a + \mathrm{cP}}{b - R * \ln \mathrm{X}_{\mathrm{TiO_2}}^{\mathrm{Qtz}} + R * \ln a_{\mathrm{TiO_2}}} - 273.15,$$

where R is the gas constant 8.3145 J/K, $\mathrm{X}_{\mathrm{TiO_2}}^{\mathrm{Qtz}}$ is the mole fraction of TiO_2 in quartz (ppm), $a_{\mathrm{TiO_2}}$ is the activity of TiO_2 in the system, and the adjustable parameters a, b, and c are $a = 60{,}952 \pm 3{,}122$, $b = 1.520 \pm 0.04$, and $c = 1{,}741 \pm 63$ (Thomas et al. 2010).

It was impossible to perform an independent pressure estimation from the available drill cuttings. Thus, a pressure of 5 kbar was used based on previous pressure estimations from the formations of the study area (Árkai and Nagy 1994, $P = 3.2$–4.0 kbar; Lelkes-Felvári et al. 2000, $P = 5.7$–6.3 kbar, Barrow-type pressure conditions). In our calculations, a TiO_2 activity of $a_{\mathrm{TiO_2}} = 1.0$ was used because anatase (TiO_2) inclusions were detected by Raman spectroscopy in most of the analyzed quartz grains (see later).

Ti concentrations and the calculated temperatures are interpreted as functions of the deformation conditions of the quartz grains. The quartz grains measured by LA-ICP-MS were also analyzed in the *F1–F2* spectral space. Isotherms in the *F1–F2* space were fitted by Golden Software Surfer using the linear kriging method.

Micro-Fourier-transform infrared (FTIR) spectroscopy measurements

Quartz grains were analyzed by FTIR. Four samples were measured along the previously localized ductile shear zone (rim: 1,605 m; core: 1,620 and 1,635 m; rim: 1,660 m; Fig. 5). During the measurement, the hydroxyl defects and molecular water content of the quartz lattice were also determined.

Unpolarized micro-FTIR measurements on unoriented quartz grains were undertaken at the Hungarian Institute for Forensic Sciences using a Bruker Vertex 70 spectrometer attached to a Bruker Hyperion 1000 infrared microscope. KBr beam splitters and mercury–cadmium–telluride detectors were deployed with a Globar light source. Measurements were conducted using unpolarized infrared light. The rectangular spot size was set at 100×100 μm. A nominal spectral resolution of 4 cm^{-1} was

chosen with at least 64 scans, usually ranging between 400 and 4,000 cm^{-1} for each measurement.

The indicatrix theory (Kovács et al. 2008; Sambridge et al. 2008) of unpolarized infrared light makes it possible to determine the concentration of anisotropic structural hydroxyl defects from a number ($n > 5$) of unoriented crystals with reasonable accuracy. This method can only be applied to strongly anisotropic minerals (e.g., olivine, calcite, and quartz), if the maximum linear unpolarized absorbance is less than 0.15, a criterion that is satisfied by the spectra measured in this study. Absorbers such as molecular water in inclusions or interstitial crystallographic positions are isotropic; therefore, a single measurement is enough for precise quantitative evaluation.

The total polarized absorbance (A_{tot}) for structural hydroxyl in quartz grains is estimated as three times that of the average integrated unpolarized absorbance (Kovács et al. 2008; Sambridge et al. 2008). The estimation of the average integrated unpolarized absorbance A_{tot} is more accurate when the number of measurements on unoriented grains is larger. In this study, sometimes only one grain was available for such analysis; consequently, the uncertainty is worse and can reach up to 30%. In the integrated area, the integration was undertaken using OPUS software for structural hydroxyl between 3,365 and 3,395 cm^{-1}. The A_{tot} was then converted to the absolute concentration of hydroxyl defects using the calibration factors of Thomas et al. (2009) for natural quartz (HQV, $\varepsilon = 94{,}000$ L/mol cm^2, $k \sim 0.072$). The approximate amount of molecular water in (nanoscale) inclusions was estimated following the methodology of Gleason and DeSisto (2008) and applying the absorption coefficient of Kats (1962) based on the integrated absorbance of the broad molecular water band at ~3,400 cm^{-1}. For this analysis, the limits of integration were set between 3,000 and 3,695 cm^{-1}. In this case, anisotropy is not a factor; therefore, the uncertainty originates solely from the heterogeneity in the concentration of molecular water.

Thicknesses of quartz wafers were determined based on the integrated area under the Si–O bands between 1,440 and 2,110 cm^{-1} as described by Bíró et al. (2016). The determined thickness of the sample, possible heterogeneities in hydroxyl defect concentrations, and the calibration factors may be all the sources of possible uncertainties. However, based on previous experience (Kovács et al. 2008, 2012), the overall precision in the absolute concentration of hydroxyl defects here should be as high as ~40%, and that of molecular water should be as high as ~15%.

Results

Raman spectroscopy

The analyzed quartz grains can roughly be divided into two groups based on their microstructures and deformation conditions. These are grains with undulose extinction (close to U) and recrystallized grains (close to R). In addition, numerous grains with

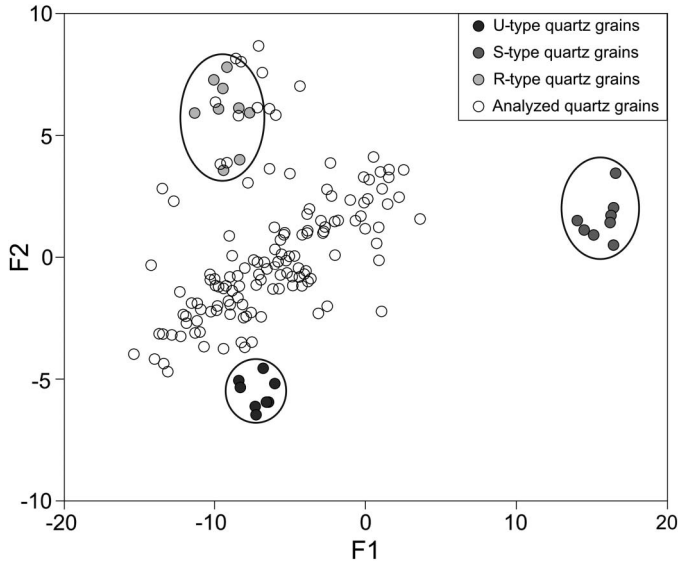

Fig. 6
Position of analyzed quartz grains in the U–S–R spectral space using Raman spectroscopy on the basis of *F1, F2* discriminant functions

heterogeneous microstructures were also observed; they exhibit the simultaneous presence of domains with U, S, and R microstructures within a single grain (Fig. 6).

Numerous tiny (up to a few microns in diameter) anatase inclusions, formed by low-temperature modification of TiO_2 minerals, were detected by Raman spectroscopy in the analyzed quartz grains. In the studied quartz grains, anatase appears as homogeneously distributed inclusions (Fig. 7).

LA-ICP-MS

Ti concentration data. In the sample from 1,675 m, Ti concentrations range between 4 and 70 ppm; in the sample from 1,770 m, Ti concentrations vary between 5 and 42 ppm. Some concentration data are below the detection limit (1 ppm).

TitaniQ thermometry

The temperature data calculated using a TitaniQ thermometer is presented as histograms (Fig. 8). In the case of the sample obtained from a depth of 1,675 m, temperatures vary between 390 and 590 °C (Fig. 8a); in the sample collected from a depth of 1,770 m, $T = 410$–547 °C (Fig. 8b). Both histograms appear to be bimodal. There in the 1,675-m sample, temperature data vary between 390 and 485 °C and

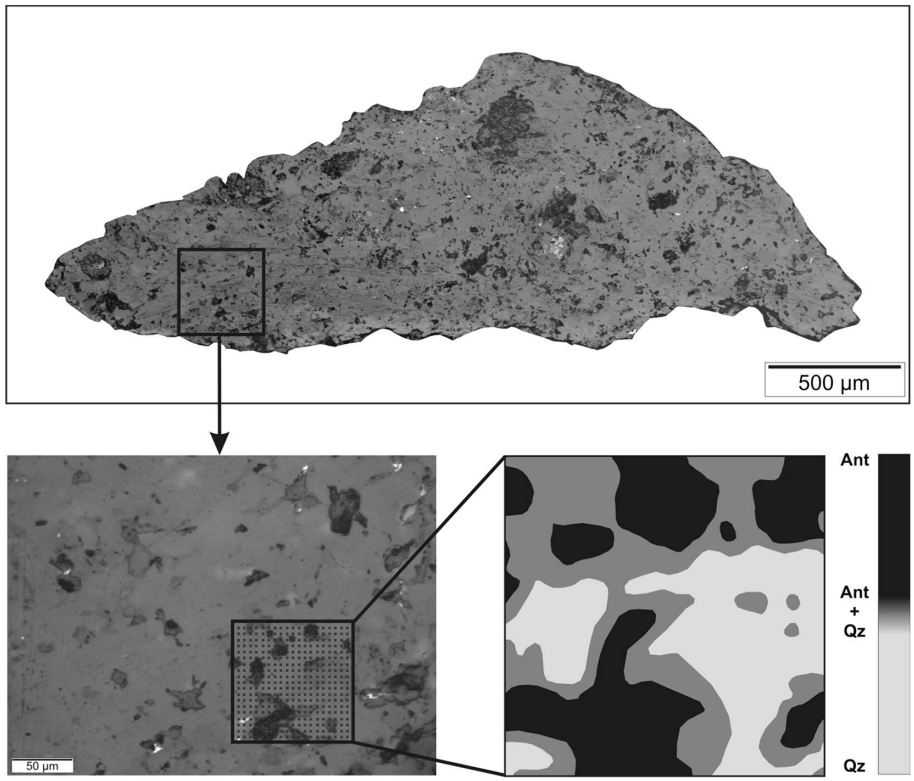

Fig. 7
Raman map of anatase inclusions in a representative quartz grain

between 500 and 590 °C, respectively, whereas there in the 1,770-m sample, it varies between 410 and 470 °C and between 500 and 550 °C, respectively.

The significant difference between the two temperature groups is also justified by two-sample (independent) *t*-tests at the 95% significance level at both depths. The bimodality of these temperature distributions suggests that both high- and low-temperature events occurred in both studied samples.

Combined Raman spectroscopy and LA-ICP-MS results

All temperature data were connected to the deformation state of the corresponding quartz grains based on their positions in the *F1–F2* spectral space (Fig. 9). In this way, temperatures of the deformation mechanisms by which these structurally different grains were formed can be estimated (Fig. 9a). This figure shows clear covariation

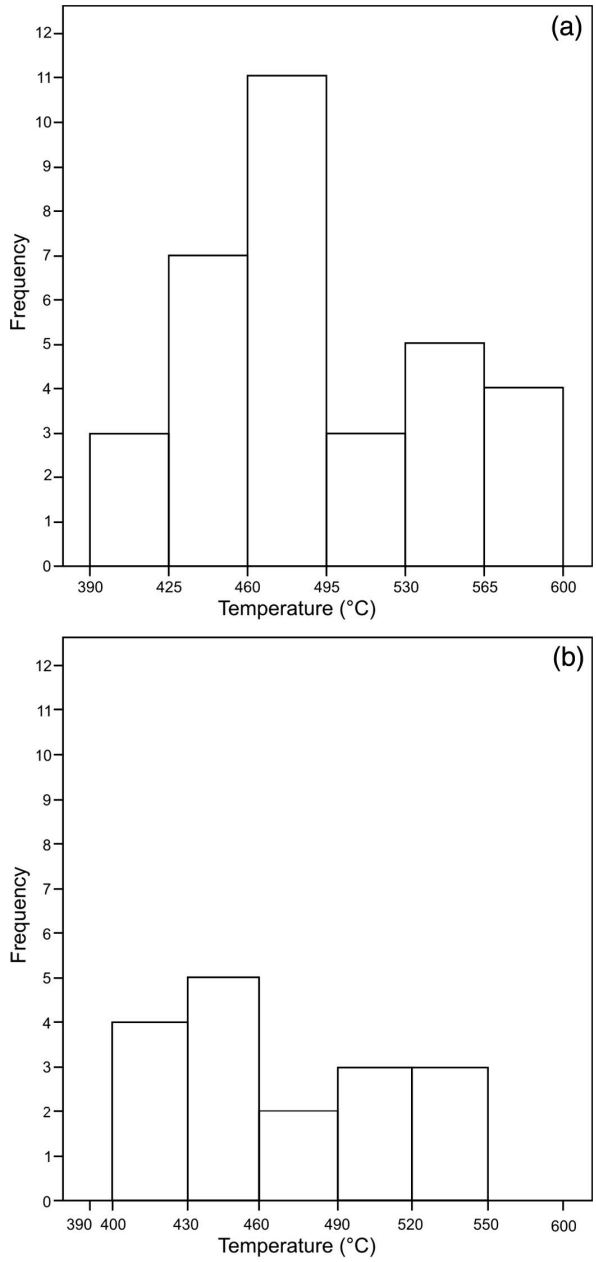

Fig. 8
Histograms of temperature data calculated using TitaniQ thermometer (Thomas et al. 2010). (a) Histogram of temperature data from a 1,675-m-deep sample and (b) histogram of temperature data from a 1,770-m-deep sample

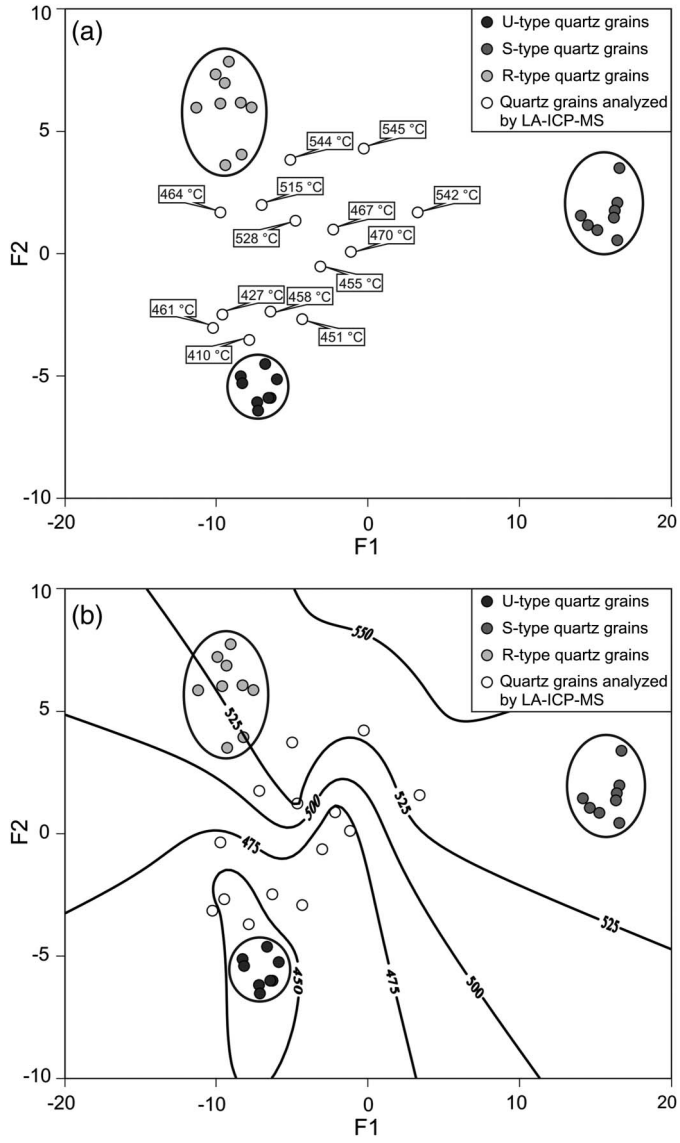

Fig. 9
Combined Raman spectroscopy and LA-ICP-MS results. (a) All temperature data (each temperature datum represents an average temperature of multiple points measured in the same quartz grain, standard deviation in each measured point is <3 °C) are connected to the deformation state of the corresponding quartz grains based on their positions in the *F1–F2* spectral space, and (b) interpolated and extrapolated isotherms display a continuous temperature decrease from R to U

between deformation state and temperature; structurally different grains contain different amounts of Ti. Grains that plot close to the U-type field contain less Ti (4–19 ppm), whereas those close to R-type grains contain higher amount of Ti (23–70 ppm). Accordingly, temperatures related to the deformation conditions represented by U are between 400 and 475 °C, whereas for deformation conditions represented by R, $T = 500$–575 °C. Moreover, interpolated and extrapolated isotherms fitted using each point with known temperatures in the U–S–R spectral space suggest a continuous temperature decrease from R to U (Fig. 9b).

Micro-FTIR results

The broadband at ~3,400 cm^{-1} usually corresponds to molecular water in inclusions or interstitial positions in quartz (Kats 1962; Stenina 2004). The concentration of molecular water varies from 357 to 1,060 ppm in the measured quartz grains (Table 1). Samples collected from depths of 1,605 and 1,660 m have significantly more molecular water than the other two samples; this difference is well-beyond analytical uncertainty (Fig. 10). There is a narrower band superimposed on the "water" band at ~3,380 cm^{-1}, which is usually attributed to the coupled substitution of $Al^{3+} + H^{+}$ for Si^{4+}. The frequency of this substitution is rather low (0.8–2.8 ppm). The samples collected from depths of 1,605 and 1,660 m also display higher concentrations of structural hydroxyl (Fig. 10, Table 1); however, due to their higher analytical uncertainty, this difference may be marginal.

Discussion

Evolution

The drill cuttings representing the gneissic rocks of the crystalline basement of the Mecsekalja Zone contain monomineralic quartz grains in addition to tiny rock grains, the latter consists essentially of quartz, K-feldspar, plagioclase, and mica (muscovite and biotite). In this quartzofeldspathic system, quartz may be a relict phase of the

Table 1
"Water" content of quartz grains along the shear zone

Depth of sample (m)	Hydroxyl defect (ppm) (Thomas et al. 2009)	Molecular water (ppm) (Kats 1962)
1,605	2.8	784
1,620	0.8	384
1,635	1.1	357
1,660	2.0	1,060

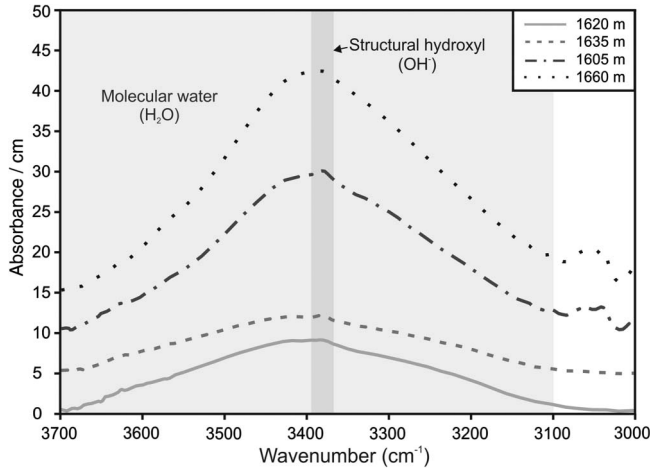

Fig. 10
IR spectra (between 3,700 and 3,000 cm^{-1}) of analyzed quartz samples from different depths along the localized ductile shear zone (rim: 1,605 m; core: 1,620 and 1,635 m; rim: 1,660 m). The wide light gray band (3,100–3,500 cm^{-1}) displays the band of molecular water (H_2O), whereas the narrow dark gray band (3,380 cm^{-1}) displays the band of structural hydroxyl (OH^-)

pre-metamorphic protolith or a product of metamorphic reactions. In the studied samples, quartz grains can be subdivided into two main groups based on their microstructures and deformation conditions. There are quartz grains with undulose extinction (U) that are formed by a BLG recrystallization mechanism. Based on TitaniQ thermometry, the temperatures related to this deformation event are 390–485 °C in the upper gneiss type and 410–470 °C in the lower zone. The other dominant grain type (R) is formed during SGR at temperatures of 500–590 °C in the upper zone and 500–550 °C in the lower gneiss zone. Based on previous studies (Hirth and Tullis 1992; Passchier and Trouw 2005, among others), in quartz, the BLG dynamic recrystallization mechanism occurs at ~400 °C, while SGR II is active at ~500 °C. These data are in accordance with the above temperature estimates for U- and R-type grains and confirm that the two subsequent deformation events occurred at different conditions.

Metamorphism and ductile deformation

In the quartz lattice, trace elements, hydroxyl defects, and molecular water may be present in various amounts (Götze et al. 2004; Stenina 2004). The incorporation of Ti into quartz during metamorphism depends only on the *P–T* conditions, provided that Ti is present in excess. An obvious textural method for determining whether sufficient amounts of Ti were present is the occurrence of anatase inclusions in each studied

grain. At a high *T*, the quartz lattice contains the highest amount of Ti, which precipitates as anatase (TiO_2) when the rock cools down. In this way, "quartz-anatase myrmekite" forms through subsolidus exsolution. The R-type quartz grains contain the highest Ti concentrations (23–70 ppm). The Ti concentrations and corresponding temperatures (500–575 °C) of these grains imply that they experienced the highest-temperature metamorphic event in the study area. The newly recrystallized R-type grains formed during coeval ductile deformation and recrystallization.

In the quartz lattice, the microtextural and chemical equilibrium states depend on the rates of dislocation migration and diffusion, respectively. The rates of both processes significantly depend on temperature and fluid content (Hirth and Tullis 1992; Fossen 2010). During BLG and SGR, dislocation migration and diffusion are usually too slow to obtain total equilibrium because of their low temperatures (<500 °C). Nevertheless, local equilibrium can be reached on the scale of some grains in terms of both microtexture and chemistry (Grujic et al. 2011; Haertel et al. 2013). In the quartz lattice, the appearance of "water" (OH^-, H_2O) causes hydrolytic weakening (Griggs and Blacic 1965; Kronenberg and Wolf 1990). Moreover, water also promotes dislocation migration and diffusion and thus may cause ductile deformation to occur at relatively low temperatures (200–300 °C; Griggs and Blacic 1965; Blacic 1975; Jones 1975; Kekulawala et al. 1978, 1981; Gleason and DeSisto 2008). Consequently, equilibrium can presumably be reached even at this physical condition. Among the studied quartz grains, the U-type grains contain the lowest concentrations of Ti (4–19 ppm). The temperature represented by these grains (400–475 °C) represents the temperature of recrystallization along the retrograde pathway.

Effect of "water" on the brittle deformation of quartz

In the localized ductile shear zone (1,610–1,635 m), the water content (OH^-, H_2O) of quartz grains decreases from the rims to the central part of the shear zone. As a consequence of intensive shear deformation, quartz grains from the central part of the shear zone became microstructurally very fine-grained. As a result, intragranular structures, containing hydroxyl defects and molecular water, were destabilized in these quartz crystals, and water, which was present in the quartz lattice before deformation, was liberated from the crystal structure (Zhou et al. 2008). Thus, in regions where quartz-suffered intensive ductile deformation (in the core part of the shear zone), the grains are partly dehydrated. In regions where quartz was not as intensively deformed (away from the shear zone), the water content (OH^-, H_2O) of the grains has been preserved.

Results of fracturing tests performed on quartz (Doukhan 1995; Kornev and Razvorotneva 1998) indicate that brittle deformation is most intensive if the quartz lattice is dry or contains only a small amount of water. Although the strength of wet quartz is an order of magnitude lower than the strength of dry quartz, the limiting deformation of wet quartz is larger than that of dry quartz (Kornev and Razvorotneva 1998). Limiting deformation is the maximum deformation that a material can carry

without failing (Protostenya et al. 2016). Nevertheless, the presence of a small amount of water in the quartz lattice reduces the stress required for fracturing (Ball and Payne 1976). Thus, brittle shear zones were able to form in rock sections that previously suffered intensive ductile deformation and became partly dehydrated.

Geodynamics

Theoretically, the coincidence of the border between different gneiss types with the depths of the ductile and brittle shear zones allows for two different interpretations regarding the structural evolution of this region. First, if the evolved ductile shear zone created softened regions inside the crystalline mass, then it could reactivate later in a brittle manner due to a tectonic event independent of the early one. On the other hand, if these structures were formed by the same tectonic event, causing ductile and brittle deformation to overlap along the same shear zones, then these zones may represent a detachment fault.

Based on the TitaniQ thermometer results, the formations above and below the shear zone display the same maximum metamorphic temperature (T_{max} = 500–575 °C) and retrograde overprint. Thus, the analyzed structural zone features the border of two rock bodies with the same metamorphic history. By definition, a detachment fault divides crystalline blocks of significantly different metamorphic evolutions; consequently, the studied shear zone is likely not a detachment fault. The coincidence of the ductile and brittle zones along the Sztl-1 well can be explained instead by the behavior of quartz. Quartz grains were dehydrated in the central part of the shear zone due to intensive ductile deformation relative to that of nearby rocks. Therefore, gneisses inside the shear zone became more rigid and ready to deform in a brittle style. Thus, in

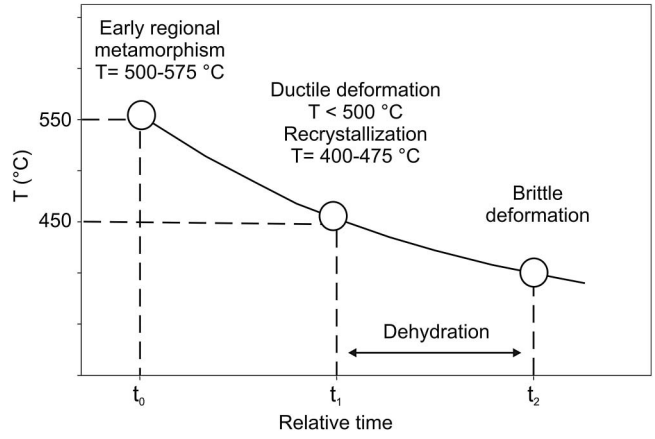

Fig. 11
Metamorphic and structural evolution of the Mecsekalja Zone around the Sztl-1 well

the studied section of the Mecsekalja Zone, there were most likely at least two independent, single, consecutive deformation events in which the ductile shear zone was reactivated in a brittle way.

Connections with previous results from the study area

Based on our results, during the metamorphic and structural evolution of the Mecsekalja Zone, the maximum temperature of early regional metamorphism was between 500 and 575 °C. The temperature of the subsequent ductile deformation was below 500 °C followed by recrystallization occurred at a temperature between 400 and 475 °C. During the structural evolution of the study area, there were at least two independent, single deformation events. The earlier ductile deformation event was followed by a brittle one through the reactivation of the former ductile shear zone (Fig. 11).

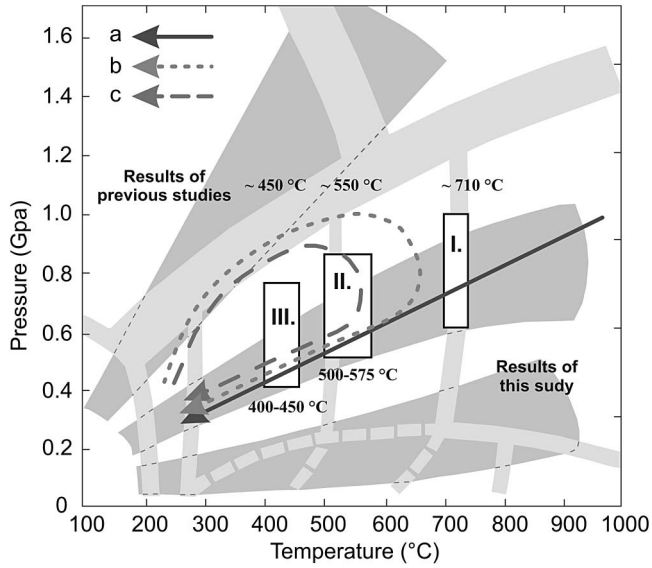

Fig. 12
Comparison of Sztl-1 well with previous results concerning the evolution of the Mecsekalja Zone. Gray fields show the main metamorphic facies series of Miyashiro (1973, 1994) and Winter (2014). a, b, and c are the development models of different rock types of the Ófalu Group: a: gneiss; b: amphibolite; c: crystalline limestone, quartz phyllite, and metasandstone. I., II., and III. are the previously defined events during the evolution of Mecsekalja Zone: I. magmatic crystallization of quartz grains of gneiss protolith granitoid rocks (~710 °C, M. Tóth et al. 2005), II. regional metamorphic event at upper greenschist/lower amphibolite facies (~550 °C, Szederkényi 1977, 1983; Árkai and Nagy 1994; Lelkes-Felvári et al. 2000; M. Tóth et al. 2005) in both gneissic rocks and amphibolites, and III. all rock types of the Ófalu Group uniformly suffered high-temperature greenschist facies regional metamorphism, mylonitization, and recrystallization (~450 °C, Szederkényi 1977, 1983; Lelkes-Felvári et al. 2000; Király and Török 2003; M. Tóth et al. 2005). Based on the current results, the early regional metamorphism (II.) occurred between 500 and 575 °C, whereas recrystallization (III.) occurred between 400 and 475 °C

The estimated temperatures of regional metamorphism (500–575 °C) display good coincidence with the previous results of Szederkényi (1977, 1983), Árkai and Nagy (1994), Lelkes-Felvári et al. (2000), and M. Tóth et al. (2005), who also estimated that greenschist/amphibolite facies metamorphism occurred at a temperature of 540–550 °C. The temperature of ductile deformation and mylonitization, <500 °C (400–475 °C), is also in good agreement with the previous results of Lelkes-Felvári et al. (2000), Király and Török (2003), and M. Tóth et al. (2005). These researchers estimated a temperature of ~500 °C for metamorphism under greenschist facies conditions and a recrystallization temperature of 350–400 °C.

Based on the detailed analysis of quartz chips from the Sztl-1 well, our schematic model is in accordance with previous results concerning the evolution of the Mecsekalja Zone (Szederkényi 1977, 1983; Árkai and Nagy 1994; Lelkes-Felvári et al. 2000; Király and Török, 2003; M. Tóth et al. 2005) (Fig. 12). Thus, previous evolution models of the Mecsekalja Zone can be extended toward the southwest, at least to the Sztl-1 well.

Acknowledgements

The authors would like to thank Mannvit Ltd. and László Ádám for providing the samples and Geo-Log Ltd. and PannErgy Plc. for geophysical data. This study was supported by a Bolyai Postdoctoral Fellowship to IJK. English was corrected by American Journal Experts. Comments of two anonymous reviewers are acknowledged.

References

Árkai, P., G. Nagy 1994: Tectonic and magmatic effects on amphibole chemistry in mylonitized amphibolites and amphibolite-bearing enclaves associated with granitoid rocks, Mecsek Mountains, Hungary. – Acta Geologica Hungarica, 37, pp. 235–268.

Ball, A., B.W. Payne 1976: The tensile fracture of quartz crystals. – Journal of Material Science, 11, pp. 731–740.

Balla, Z. 2003a: Ófalui Formáció, paleozoikum [Ófalu Formation, Palaeozoic]. – In: Balla, Z. (Ed): Az atomerőművi kis és közepes aktivitású radioaktív hulladékok végleges elhelyezésére irányuló program. A felszíni földtani kutatás zárójelentése, Bátaapáti, Üveghuta [Program for the Final Disposal of Low and Medium Level Radioactive Waste. Final Geological Report of the Ground-Based Geological Exploration, Bátaapáti, Üveghuta]. – Manuscript, Geological Institute of Hungary, Budapest, Hungary, pp. 103–105. (in Hungarian)

Balla, Z. 2003b: Magmás képződmények (Magmatic sequences). – In: Balla, Z. (Ed): Az atomerőművi kis és közepes aktivitású radioaktív hulladékok végleges elhelyezésére irányuló program. A felszíni földtani kutatás zárójelentése, Bátaapáti, Üveghuta [Program for the Final Disposal of Low and Medium Level Radioactive Waste. Final Geological Report of the Ground-Based Geological Exploration, Bátaapáti, Üveghuta]. – Manuscript, Geological Institute of Hungary, Budapest, Hungary, pp. 109–112. (in Hungarian)

Balla, Z., G. Császár, Z. Gulácsi, L. Gyalog, M. Kaiser, E. Király, L. Koloszár, B. Koroknai, Á. Magyari, Gy. Maros, I. Marsi, P. Molnár, Á. Rotárné Szalkai, Gy. Tóth 2009: A Mórágyi-rög északkeleti részének földtana [Geology of the North-Eastern Part of the Mórágy Block]. – Magyar Állami Földtani Intézet, Budapest, 283 p.

Blacic, J. D. 1975: Plastic-deformation mechanisms in quartz: The effect of water. – Tectonophysics, 27, pp. 271–294.

Bíró, T., I.J. Kovács, E. Király, Gy. Falus, D. Karátson, Zs. Bendő, T. Fancsik, J.K. Sándorné 2016: Concentration of hydroxyl defects in quartz from various rhyolitic ignimbrite horizons: Results from unpolarized micro-FTIR analyses on unoriented phenocryst fragments. – European Journal of Mineral, 28, pp. 313–327.

Davis, G.A. 1988: Rapid upward transport of mid-crustal mylonitic gneisses in the footwall of a Miocene detachment fault, Whipple Mountains, southeastern California. – Geologische Rundschau, 77/1, pp. 191–209.

Doukhan, J. 1995: Lattice defects and mechanical behaviour of Quartz SiO2. – Journal de Physique III, EDP Sciences, 5/11, pp. 1809–1832.

Fossen, H. 2010: Structural geology. – Cambridge University Press, New York, NY, 481 p.

Gleason, G., S. DeSisto 2008: A natural example of crystal-plastic deformation enhancing the incorporation of water into quartz. – Tectonophysics, 446, pp. 16–30.

Götze, J., Plötze, M., Graupner, T., Hallbauer, D.K., Bray, C.J. (2004): Trace element incorporation into quartz: A combined study by ICP-MS, electron spin resonance, cathodoluminescence, capillary ion analysis, and gas chromatography. Geochimica et Cosmochimica Acta, 68/18, pp. 3741–3759.

Griggs, D. T., J. D. Blacic 1965: Quartz: Anomalous weakness of synthetic crystals. – Science, 147, pp. 292–295.

Grujic, D., M. Stipp, J.L. Wooden 2011: Thermometry of quartz mylonites: Importance of dynamic recrystallization on Ti-in-quartz reequilibration. – Geochemistry, Geophysics, Geosystems, 12/6, p. Q06012.

Haertel, M., M. Herwegh, T. Pettke 2013: Titanium-in-quartz thermometry on synkinematic quartz veins in a retrograde crustal-scale normal fault zone. – Tectonophysics, 608, pp. 468–481.

Halfpenny, A., D.J. Prior, J. Wheeler 2012: Electron backscatter diffraction analysis to determine the mechanisms that operated during dynamic recrystalisation of quartz-rich rocks. – Journal of Structural Geology, 36, pp. 2–15.

Hirth, G., J. Tullis 1992: Dislocation creep regimes in quartz aggregates. – Journal of Structural Geology, 14, pp. 145–159.

Holdsworth, R.E., C.A. Butler, A.M. Roberts 1997: The recognition of reactivation during continental deformation. – Journal of Geological Society of London, 154, pp. 73–78.

Jones, M.E. 1975: Water weakening of quartz, and its application to natural rock deformation. – Journal of Geological Society of London, 131, pp. 429–432.

Kats, A. 1962: Hydrogen in alpha-quartz. – Philips Research Reports, 17/1–31, pp. 133–279.

Kekulawala, K.R.S.S., M.S. Paterson, J.N. Boland 1978: Hydrolytic weakening in quartz. – Tectonophysics, 46, pp. T1–T6.

Kekulawala, K.R.S.S., M.S. Paterson, J.N. Boland 1981: An experimental study of the role of water in quartz deformation. – Geophysical Monograph Series, 24, pp. 49–60.

Kempe, U., J. Götze., E. Dombon, T. Monecke, M. Poutivtsev 2012: Quartz regeneration and its use as a repository of genetic information. In: J. Götze, R. Möckel (eds.), Quartz: Deposits, Mineralogy and Analytics. Springer, Berlin/Heidelberg, Germany, pp. 313–355.

Király, E. 2005: Microscopic description of the field samples. – Manuscript, MÁFI, Tekt, Budapest, p. 1242.

Király, E., K. Török 2003: Magmatic garnet in deformed aplite dykes from the Mórágy granitoid, SE-Transdanubia. – Acta Geologica Hungarica, 46/3, pp. 239–254.

Klötzli, U.S., Gy. Buda, T. Skiold 2004: Zircon typology, geochronology and whole rock Sr-Nd isotope systematics of the Mecsek Mountain granitoids in the Tisia Terrane (Hungary). – Mineralogy and Petrology, 81/1–2, pp. 113–134.

Konrád, Gy., K. Sebe, A. Halász, E. Babinszki 2010: Sedimentology of Permian playa lake: The Boda Claystone Formation, Hungary. – Geologos, 16/1, pp. 27–41.

Kornev, V.M., L.I. Razvorotneva 1998: Comparative estimates of the strength of dry and wet quartz in griding. – Journal of Applied Mechanics and Technical Physics, 39/1, pp. 121–125.

Kovács, I., D. Green, A. Rosenthal, J. Hermann, H.St.C. O'Neill, W.O. Hibberson, B. Udvardi 2012: An experimental study of water in nominally anhydrous minerals in the upper mantle near the water saturated solidus. – Journal of Petrology, 53, pp. 2067–2093.

Kovács, I., J. Hermann, H.St.C. O'Neill, J. D. FitzGerald, M. Sambridge, G. Horváth 2008: Quantitative absorbance spectroscopy with unpolarized light, Part II: Experimental evaluation and development of a protocol for quantitative analysis of mineral IR spectra. – American Mineralogist, 93, pp. 765–778.

Kronenberg, A.K., G.H. Wolf 1990: Fourier transform infrared spectroscopy determinations of intragranular watercontent in quartz-bearing rocks: Implications for hydrolytic weakening in the laboratory and within the earth. – Tectonophysics, 172, pp. 255–271.

Lelkes-Felvári, Gy., P. Árkai, W. Frank, G. Nagy 2000: Late Variscan ultramylonite from the Mórágy Hills, SE Mecsek Mts., Hungary. – Acta Geologica Hungarica, 43/1, pp. 65–84.

Lister, G.S., G.A. Davis 1989: The origin of metamorphic core complexes and detachment faults formed during Tertiary continental extension in the northern Colorado River region, USA. – Journal of Structural Geology, 11/1–2, pp. 65–94.

Lister, G.S., M.A. Etheridge, P.A. Symonds 1986: Application of the detachment fault model to the formation of passive continental margins. – Geology, 14, pp. 246–250.

Liu, Y., Z. Hu, S. Gao, D. Günther, J. Xu, C. Gao, H. Chen 2008: In situ analysis of major and trace elements of anhydrous minerals by LA-ICP-MS without applying an internal standard. – Chemical Geology, 257, pp. 34–43.

M. Tóth, T., G. Kovács, F. Schubert, V. Dályay 2005: Az ófalui "migmatit" eredete és deformációtörténete [Origin and deformation history of the Ófalu "migmatite"]. – Földtani Közlöny 135/3, pp. 331–352. (in Hungarian)

Miyashiro, A. 1973: Metamorphism and Metamorphic Belts. – Allen & Unwin, London, 492 p.

Miyashiro, A. 1994: Metamorphic Petrology. – UCL Press, London, 404 p.

Monecke, T., U. Kempe, J. Götze 2002: Genetic significance of the trace element content in metamorphic and hydrothermal quartz: A reconnaissance study. – Earth and Planetary Science Letters, 202, pp. 709–724.

Passchier, C.W., R.A.J. Trouw 2005: Microtectonics. – Springer-Verlag, Berlin/Heidelberg, Germany, 371 p.

Protostenya, A.G., M.A. Karasev, D.N. Petrov 2016: Investigating mechanical properties of argillaceous grounds in order to improve safety of development of megalopolis underground space. – International Journal of Applied Engineering Research, 11/16, pp. 8949–8956.

Sambridge, M., J.D. Fitz Gerald, I. Kovács, H.St.C. O'Neill, J. Hermann 2008: Quantitative IR spectroscopy with unpolarized light, Part I: Physical and mathematical development. – American Mineralogist, 93, pp. 751–764.

Skultéti, Á., T.M. Tóth 2016: Localisation of ductile and brittle shear zones along the Szentlőrinc-1 well in the Mecsekalja Zone using quartz microstructural and well-log data. – Acta Geodaetica et Geophysica, 51/2, pp. 295–314.

Skultéti, Á., T.M. Tóth, K. Fintor, F. Schubert 2014: Deformation history reconstruction using single quartz grain Raman microspectroscopy data. – Journal of Raman Spectroscopy, 45/4, pp. 314–321.

Sørensen, B.E., R.B. Larsen 2009: Coupled trace element mobilisation and strain softening in quartz during retrograde fluid infiltration in dry granulite protoliths. – Contributions to Mineralogy and Petrology, 157, pp. 147–161.

Stadler, R., J. Konzett 2012: OH defects in quartz in the system quartz-albite-water and granite-water between 5 and 25 kbar. – Physics and Chemistry of Minerals, 39, pp. 817–827.

Stenina, N.G. 2004: Water related defects in quartz. – Bulletin of Geosciences, 79, pp. 251–268.

Stipp, M., H. Stünitz, R. Heilbronner, S.M. Schmid 2002: The eastern Tonale fault zone: A 'natural laboratory' for crystal plastic deformation of quartz over a temperature range from 250 to 700°C. – Journal of Structural Geology 24, pp. 1861–1884.

Szederkényi, T. 1977: Geological evolution of South Transdanubia (Hungary) in Paleozoic time. – Acta Mineralogica-Petrographica 23/1, pp. 3–14.

Szederkényi, T. 1983: Origin of amphibolites and metavolcanics of crystalline complexes of South Transdanubia, Hungary. – Acta Geologica Hungarica, 26, pp. l03–136.

Thomas, J.B., E.B. Watson, F.S. Spear, P.T. Shemella, S.K. Nayak, A. Lanzirozzi 2010: TitaniQ under pressure: The effect of pressure and temperature on the solubility of Ti in quartz. – Contributions to Mineralogy and Petrology 160, pp. 743–759.

Thomas, S.-M., M. Koch-Müller, P. Reichart, D. Rhede, R. Thomas, R. Wirth, S. Matsyuk 2009: IR calibrations for water determination in olivine, r-GeO2, and SiO2 polymorphs. – Physics and Chemistry of Minerals, 36, pp. 489–509.

Thorbergsdottir, I.M., H. Tulinius, L. Ádám, G. Gudmundsson, H.B. Halldórsdottir, S. Traustason, Z. Hu, G. Yu 2010: Geothermal drilling for space heating in the town of Szentlőrinc in SW Hungary. – Proceedings World Geothermal Congress, Bali, pp. 1–5.

Tüske, T. 2001: A Mórágyi-rög metamorfitjainak szerkezeti értékelése (szakdolgozat) (in Hungarian, translated title: Tectonic interpretation of the metamorphism of the Mórágy Block [graduate thesis]. – Kézirat (manuscript), ELTE Természettudományi Kar, Általános és Történeti Földtan Tanszék, Budapest, 85 p.

Vernon, R.H. 2004: A practical guide to Rock Microstructure. – Cambridge University Press, Cambridge, UK, 650 p.

White, S.H., P.G. Bretan, E.H. Rutter 1986: Fault-zone reactivation: Kinematics and mechanisms. – Philosophical Transactions of the Royal Society, A317, pp. 81–97.

Winter, J.D. 2014: Principles of Igneous and Metamorphic Petrology. – Pearson, London, 745 p.

Zhou, Y., C. He, X. Yang 2008: Water contents and deformation mechanism in ductile shear zone of middle crust along Red River fault in southwestern China. – Science in China Series D: Earth Sciences, 51/10, pp. 1141–1425.